RSC Advances

PAPER

View Article Online
View Journal | View Issue

Cite this: *RSC Adv.*, 2026, **16**, 8593

Effect of different leaching agents on the recycling of valuable metals in spent molybdenum-based catalyst

Xiaoxue Sun, Deju Wang,* Junlin Zheng, Renjie Li and Fenglei Xi

Conventional hydrometallurgical recycling of spent molybdenum-based catalysts is often constrained by a trade-off between selectivity and total metal recovery when using single-step alkaline or acidic leaching. To overcome this limitation, this work presents a novel two-stage leaching process designed for the sequential and selective extraction of valuable metals. The approach leverages an initial alkaline leach (NaOH) to selectively dissolve molybdenum and silicon, achieving extraction efficiencies of 95.8% for Mo and 58.1% for Si while minimizing co-dissolution of other metals. The resulting residue is subsequently subjected to an acidic leach (HNO_3) for the comprehensive dissolution of residual Fe, Mg, Mo, and Ni. A solvent extraction step employing P507 then enables highly efficient separation, extracting 96.0% Fe and 98.4% Mo from the mixed acidic leachate. The final step uses hydrochloric acid as a stripping agent to separate Fe from Mo. This integrated methodology demonstrates a significant advancement by synergistically combining the high selectivity of alkaline media with the broad dissolution capability of acids, offering a targeted and efficient route for the valorization of complex spent catalyst streams.

Received 3rd January 2026
Accepted 30th January 2026

DOI: 10.1039/d6ra00053c

rsc.li/rsc-advances

1 Introduction

Molybdenum-based catalysts are widely utilized in various reactions, including hydrogenation, dehydrogenation, oxidation and alkylation in the fields of petrochemical and environmental protection.[1–3] The most prevalent catalysts comprise Mo oxides and other metal oxides on an alumina or silicon oxide support.[4] However, due to their limited service life, substantial quantities of spent catalysts must be replaced by fresh catalysts annually. Upon completion of their operational life, catalysts are withdrawn from the process and are subsequently classified as "spent". The regenerability of spent catalysts can be evaluated based on established methods.[5] Those deemed unsuitable for regeneration are typically destined for landfill. Inadequate management practices during disposal, however, pose a risk of heavy metal leaching, which can result in significant environmental contamination and public health hazards.[6–8] Nevertheless, spent molybdenum-based catalysts can be considered secondary resources as they contain 10%–30% Mo,[4] which is significantly higher than the Mo content in molybdenite, one of the most important primary sources of molybdenum, which contains less than 3% Mo.[9] The extraction of Mo from molybdenite through direct oxidation roasting, converting sulfide to oxide, and the subsequent leaching process is well-established in industrial applications.[10] Consequently, it can be anticipated that Mo recovery from spent catalysts is more feasible than that from molybdenite, not only due to its higher Mo content but also because of the oxide state of Mo in spent catalysts.

The extraction of metals from spent catalysts can be accomplished *via* hydrometallurgical or pyrometallurgical methods following pretreatment.[11] Hydrometallurgical approaches offer greater flexibility, containment, and value addition when handling complex raw materials.[12] Predominantly, investigations into metal recovery from spent metal catalysts involve leaching processes utilizing solutions comprising both inorganic and organic agents.[13] Research on molybdenum leaching from industrial waste has gained considerable traction since the 1970s.[4] A range of Mo leaching reagents, including inorganic acids,[14] organic acids,[14,15] and inorganic bases,[16] are employed due to the amphoteric nature of MoO_3. The aqueous solubility of Mo can be markedly enhanced through the roasting of spent catalysts with compounds containing alkali metals, such as NaOH,[17] Na_2CO_3,[18] and $KHSO_4$.[19] Alkaline roasting temperatures can reach 600 °C–800 °C, resulting in substantial energy consumption. Furthermore, the sublimation of MoO_3 during the roasting process leads to the loss of valuable elements. Consequently, there is a pressing need to develop an innovative recovery process that eliminates the roasting step.

Conventional recovery methods face a fundamental trade-off between efficiency and sustainability, as they either struggle to

State Key Laboratory of Green Chemical Engineering and Industrial Catalysis, Sinopec Shanghai Research Institute of Petrochemical Technology Co., Ltd, Shanghai, 201208, China. E-mail: wangdj.sshy@sinopec.com

liberate bound molybdenum (direct acid leaching) or high energy and environmental costs (alkali-roasting), as summarized in Table 1. To overcome these limitations, this study proposes a novel two-stage process centered on an initial selective alkaline leach, which directly extracts the majority of Mo under mild conditions, thereby enabling efficient and cleaner recovery. Key factors influencing the leaching efficiency are systematically investigated.

2 Materials and methods

2.1 Materials and reagents

All chemical reagents were used as received without further purification. Sodium hydroxide (NaOH), ammonia ($NH_3 \cdot H_2O$), ammonium carbonate ($(NH_4)_2CO_3$), ammonium nitrate (NH_4NO_3), tri-*n*-butyl phosphate (TBP), hydrochloric acid (HCl) and nitric acid (HNO_3) were purchased from Sinopharm Chemical Reagent Co., Ltd (China). The extractants 2-ethylhexyl phosphonic acid mono-2-ethylhexyl ester (P507) and di-(2-ethylhexyl) phosphoric acid (P204) were supplied by Shanghai Aoke Industrial Co., Ltd (China). Tertiary amine (N235) and sulfonated kerosene (SK) were provided by Shanghai Rare-Earth Chemical Co., Ltd (China). Cation-exchange resin 732 (a strongly acidic styrene-based resin) was purchased from Sinopharm Shanghai yuanye Bio-Technology Co., Ltd. Prior to use, the resin was soaked in four bed volumes of 1 mol L^{-1} HCl for 24 h and then rinsed with deionized water until the effluent reached pH 7.

The spent molybdenum-based catalyst was supplied by a catalyst manufacturer. Its chemical composition, as determined by inductively coupled plasma optical emission spectrometry (ICP-OES, Varian 725-ES), was 23.45% Mo, 23.6% Si, 6.16% Ni, 1.94% Fe, and 1% Mg. The catalyst was sieved through a 100-mesh sieve and calcined at 550 °C for 4 h to remove surface organic compounds.

2.2 Characterization

X-ray diffraction (XRD) patterns were obtained using a D/max 2550V (Rigaku Corporation, Japan). The purity of the silicomolybdic acid was determined by XRF analysis using a Thermo ARL ADVANT'X 2290 spectrometer (Thermo Fisher Scientific, USA).

2.3 Leaching experiments

Leaching experiments were performed in 100 mL Teflon-lined hydrothermal reactors. Eight grams of calcined spent catalyst and a certain volume of leaching agent were added to the hydrothermal reactors. Afterwards, the reactors would be installed into a homogeneous reactor (JF-8, Shanghai Lihua Instrument Equipment Co., Ltd) with rotate speed of 150 rpm. After leaching, the mixtures were filtered and washed. The content of Fe, Mg, Mo, Ni and Si in the filter residue was determined by ICP-OES, and extraction of each element was calculated using the amount in the filtrate divided by the amount in the raw materials. All leaching experiments were performed in triplicate, with the reported efficiencies representing the arithmetic mean values. In scale-up experiment, a 10 L hydrothermal autoclave was used to verify the performance of the first stage under optimal conditions. Eight hundred grams of calcined spent catalyst and 8 L NaOH (3 mol L^{-1}) were added to the reactor and then the mixture was reacted at 90 °C for 2 hours. After solid–liquid separation, the filtrate was pumped into a sand-core chromatography column to reduce Na^+ concentration.

2.4 Solvent extraction and stripping studies

Liquid–liquid extraction of Mo and Fe from the HNO_3 leaching filtrate and the corresponding stripping process were studied in 200 mL globe-shaped funnels by mixing 50 mL each of the aqueous and organic phases for predetermined periods of time at 500 rpm. The emulsion was then statically separated for 20 min, after which samples of the aqueous phase were withdrawn for analysis. Metal extraction (E) was calculated using the

Table 1 A comparative overview of recovery processes for spent hydroprocessing catalysts (high in Mo and Si)

Aspect	Proposed two-stage process	Conventional single-stage acid leaching	Conventional roasting–leaching
Core strategy	Sequential selective leaching: alkaline (for Mo, Si) → acidic (for Ni, Fe)	One-pot dissolution in strong acid (*e.g.*, H_2SO_4, HNO_3)	High-temperature fusion (with Na_2CO_3/NaOH) → water leaching
Silicon management	Valorized: selectively extracted in alkaline stage, recovered as product	Remains insoluble in the solid residue, but can encapsulate Mo, hindering its release	Controlled & solubilized: converted to soluble silicate, avoiding gelation but consuming alkali
Molybdenum recovery	High efficiency & purity *via* selective alkaline extraction and solvent extraction	Low to moderate efficiency: Co-dissolves with impurities	High efficiency, but risks volatilization loss at high roasting temperatures
Energy intensity	Moderate	Low to moderate	Very high: energy for sustained roasting (600 °C–800 °C)
Gas emissions	Negligible	Minimal: potential acid fumes	Severe
Overall character	A targeted, aqueous solution balancing efficiency and environmental impact	A problematic route for high-Si feeds due to the intrinsic silica gel issue	An energy- and emission-intensive route that externalizes the silicon problem *via* high temperature

amount of metal in organic phase divided by the amount of total metal. Distribution ratio (D) was calculated as a concentration of metal present in the organic phase to that in the aqueous phase at equilibrium. The separation factor (β) is one D divided by another, which measures the ability of the system to separate two solutes.[20]

3 Results and discussion

3.1 Pre-leaching

In traditional hydrometallurgical methods, spent catalysts are initially calcined to convert metal sulfides to metal oxides and then leached using a base or acid. Mo extraction and selectivity of one stage are usually not very high in the current study, especially in conditions dealing with raw material with complex elements. Fig. 1 shows the results of extraction with different leaching agents at 90 °C with 1 : 10 g mL^{-1} of solid-to-liquid ratio and 1 h of reaction time. HNO_3 (Fig. 1(a)) can extract most metal element in spent catalyst. Extraction of Fe, Mg, Mo and Ni reached more than 95% with 3 mol L^{-1} HNO_3 as leaching agent. This indicates that HNO_3 has no selectivity to most metals in catalyst. The effect of $NH_3 \cdot H_2O$ concentration on metal extraction was studied in the range of 0.2 mol L^{-1}~12 mol L^{-1} (Fig. 1(b)). As the concentration of $NH_3 \cdot H_2O$ increased in the range from 0.2 mol L^{-1} to 12 mol L^{-1}, it was discovered that the extraction of Mo and Ni increased significantly with $NH_3 \cdot H_2O$ concentration raised from 0.2 mol L^{-1} to 2 mol L^{-1} and then changed very little subsequently. Specifically, Mo extraction increased from 58% to 91.7%, while Ni extraction increased from 12.4% to 87.9%. MoO_3 reacted with $NH_3 \cdot H_2O$ to produce $(NH_4)_2MoO_4$, while NiO was extracted in the form of $Ni(NH_3)_6^{2+}$, $Ni(NH_3)_5^{2+}$, and in a small amount of $Ni(NH_3)_4^{2+}$.[21] Mg extraction decreased with increase in $NH_3 \cdot H_2O$ concentration because of $Mg(OH)_2$ generation. Fe and Si extraction were less than 20% over the range of $NH_3 \cdot H_2O$ concentration considered. Fig. 1(c) shows results of extraction with $(NH_4)_2CO_3$ as leaching agent with concentration ranging from 0.2 mol L^{-1} to 1 mol L^{-1}. The results of Fe, Mo and Ni extraction exhibit a similar trend as shown in Fig. 1(b). However, the extraction of Mg was much higher. Mg could be recovered from slag by carbonation process,[22] which explained the higher Mg extraction leached by $(NH_4)_2CO_3$. Experiments on metal extraction using NaOH as leaching agent were carried out and the results were presented in Fig. 1(d). The Mo and Si extraction increased with the elevation in NaOH concentration from 0.5 mol L^{-1} to 4 mol L^{-1}. The other elements (Fe, Mg and Ni) showed low extraction even when NaOH concentration reached 4 mol L^{-1}. Based on the above results, it can be concluded that NaOH and $NH_3 \cdot H_2O$ are suitable leaching agents for spent catalyst because of their high selectivity for extracting Mo. Mo extraction was higher by NaOH so NaOH leaching was studied for follow-up research. Equations for the Mo and Si leaching reactions are as follows:

$$MoO_3 + 2OH^- \rightarrow MoO_4^{2+} + H_2O \quad (1)$$

$$SiO_2 + 2OH^- \rightarrow SiO_3^{2+} + H_2O \quad (2)$$

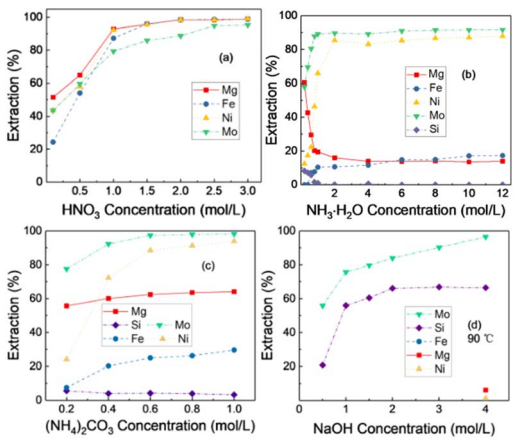

Fig. 1 Effect of different leaching solutions, namely HNO_3 (a), $NH_3 \cdot H_2O$ (b), $(NH_4)_2CO_3$ (c) and NaOH (d).

3.2 First-stage leaching

3.2.1 Laboratory-scale experiment. Firstly, the leaching process was optimized and the examined experimental factors were as follows: temperature, NaOH concentration, solid-to-liquid ratio, and reaction time. While considering one factor, the other factors were maintained constant at 90 °C for temperature, 3 mol L^{-1} for NaOH concentration, 1 : 10 for solid-to-liquid ratio, and 1 h for reaction time.

The leaching behavior of the spent catalyst was investigated across a temperature range of 80–120 °C and NaOH concentrations of 0.5 mol L^{-1}–4 mol L^{-1}. As illustrated in Fig. 1(d) and 2, elevated temperature and NaOH concentration generally enhanced the extraction of multiple elements. At 80 °C, the leaching rate of Mo was kinetically limited, resulting in an extraction efficiency below 90%; achieving 90% recovery at this temperature would require significantly prolonged reaction time, thereby increasing the cumulative thermal energy input per unit of product. In contrast, temperatures above 90 °C, while accelerating Mo extraction, induced substantial co-dissolution of Fe, Mg, and Ni—a phenomenon exacerbated by excessive NaOH. This loss of selectivity would necessitate energy-intensive downstream separation steps to purify the Mo product, largely transferring and amplifying the energy cost to subsequent unit operations. Therefore, 90 °C was selected as the optimal operating temperature because it represents the point of minimum total process energy consumption. It ensures sufficiently fast and complete Mo extraction (>90%) in a single leaching step while maintaining high selectivity, thereby avoiding the energy penalties associated with either extended leaching time or complex impurity removal processes.

Fig. 3 presents the extraction efficiencies of Mo and Si as functions of the solid-to-liquid ratio and reaction time at 90 °C using 3 mol L^{-1} NaOH. The leaching of both elements increased with prolonged time but exhibited a pronounced inverse relationship with the solid-to-liquid ratio. As the solid-to-liquid

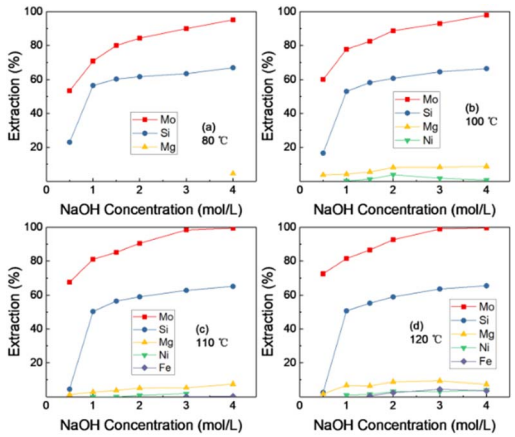

Fig. 2 Effect of temperature (80 °C (a), 100 °C (b), 110 °C (c) and 120 °C (d)) and NaOH concentration on extraction.

ratio decreased from 1 : 1 to 1 : 20 (g mL^{-1}), Mo extraction increased drastically from 51.7% to 96.1%, while Si extraction grew moderately from 54.2% to 65.9%. This drastic enhancement is primarily attributed to the alleviation of severe mass transfer limitations at high solid-to-liquid ratios. A low liquid volume (*e.g.*, solid-to-liquid ratio of 1 : 1) results in viscous slurry, poor mixing, and the rapid depletion of OH^- ions at the solid–liquid interface, which collectively inhibit the dissolution kinetics. Increasing the liquid volume improves diffusion, maintains a stable reactant concentration, and shifts the local chemical equilibrium favorably. Based on this trend, a solid-to-liquid ratio of 1 : 10 was selected as the optimal condition, yielding high Mo extraction while maintaining manageable Si co-dissolution. This condition effectively overcomes the kinetic barriers observed at 1 : 1, without incurring the diminishing returns and excessive reagent consumption associated with higher dilution. While Mo extraction reached 95.7% at 120 min, Si extraction was less sensitive to time. Consequently, the optimized parameters for scale-up were established as 90 °C, 3 mol L^{-1} NaOH, a 2 h reaction time, and a solid-to-liquid ratio of 1 : 10 g mL^{-1}.

3.2.2 Kinetic analysis. To elucidate the kinetic behaviour of molybdenum (Mo) extraction from spent catalyst *via* alkaline leaching, the experimental data were analysed using the JANDER model[23] (eqn (3)), which exhibited the highest correlation (R^2), after testing several kinetic models,

$$[1 - (1 - \alpha)^{1/3}]^2 = kt \quad (3)$$

where α is the fraction of Mo leached (%), k is the apparent rate constant (min^{-1}), and t is the reaction time (min). Experiments were conducted at four temperatures: 70 °C, 80 °C, 90 °C, and 100 °C (Fig. 4). The activation energy E_a was calculated using the Arrhenius equation, $k = A\exp(-E_a/RT)$, where R is 8.314 J mol^{-1} K^{-1} and T is the absolute temperature. A plot of ln k *versus* $1/T$ showed a linear relationship with a slope of −2933.6 K, corresponding to an activation energy of 24.4 kJ mol^{-1}. This low activation energy suggests that the leaching process is diffusion-controlled, which is in consistent with the JANDER model.

3.2.3 Scale-up testing. In scale-up experiment, 95.8% Mo and 58.1% Si were extracted from the raw material with no other elements found in the filtrate. Result of scale-up experiment was inconsistent with that of laboratory experiment. Fig. 5 displays the XRD spectra of calcined spent catalyst and its NaOH leaching residue. The major peaks in the XRD pattern of calcined catalyst correspond to $NiMoO_4$, $MgMoO_4$, and $Fe_2(MoO_4)_3$. The intensity of all peaks was reduced after NaOH leaching, indicating that part of Mo had been leached out. The other elements, namely Fe, Mg, and Ni, were not extracted and might be in the form of hydroxide.

SEM-EDS elemental mapping was performed to investigate the distribution of key metals before and after alkaline leaching. As shown in Fig. 6, prior to NaOH treatment, distinct mapping signals were obtained for Mo, Si, Ni, and Mg, confirming their presence and dispersion in the raw catalyst. Notably, no clear Fe mapping signal was detected in the unleached sample, which may be attributed to its low concentration, its incorporation into poorly crystalline or amorphous phases. Following alkaline leaching, Mo mapping signals were virtually absent in the residue, providing direct visual evidence that the majority of molybdenum was successfully dissolved, consistent with the high extraction efficiency of 95.8%. Concurrently, the intensity and distribution of the Si signal were observed to decrease, in consistent with the partial leaching of silicon (58.1% extraction). These mapping results visually corroborate the selective dissolution of Mo and the substantial removal of Si during the NaOH leaching stage.

For the scale-up experiment, the filtrate containing 24.4 g L^{-1} Mo, 13 g L^{-1} Si, and 63.25 g L^{-1} Na was pumped into a sand-core chromatography column filled with cation-exchange resin 732 from the bottom. The exchange fluid underwent evaporative crystallization to produce silicomolybdic acid. The purity of the

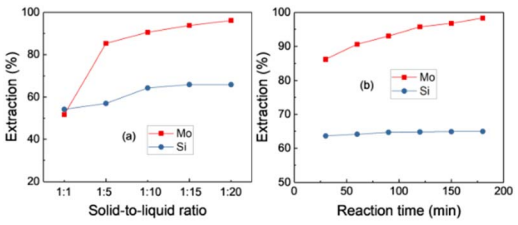

Fig. 3 Effect of solid-to-liquid ratio (a) and reaction time (b) on Mo and Si extraction.

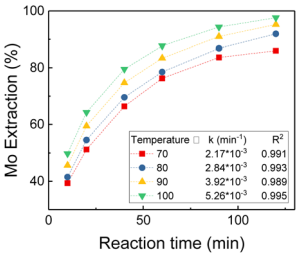

Fig. 4 Mo extraction as a function of time.

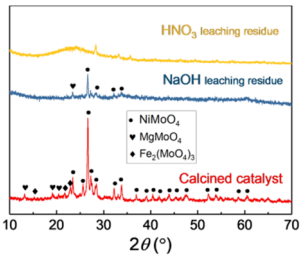

Fig. 5 X-ray diffraction patterns of fresh catalyst and leaching residues.

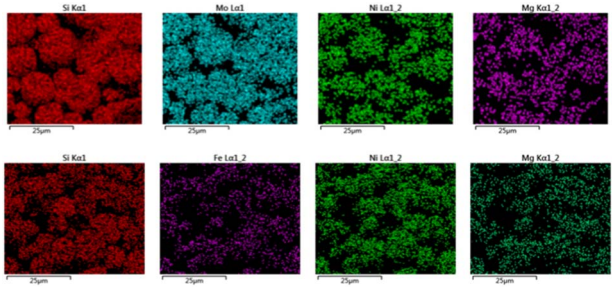

Fig. 6 Element map of fresh catalyst (up) and NaOH leaching residues (down).

silicomolybdic acid was determined by XRF analysis, which showed that only 0.055% Na_2O was present in the silicomolybdic acid, indicating good Na^+ exchange performance of the cation-exchange resin 732.

3.3 Second-stage leaching

The NaOH leaching residue, which accounts for approximately 40% of original raw material, still contains valuable elements such as Fe, Mg, Mo, and Ni, and requires secondary leaching.

As described in Fig. 1, it was found that HNO_3 could extract all of the metal elements present in the spent catalyst. Therefore, for the second-stage leaching, we adopted HNO_3. Eqn (4)–(7) correspond to the HNO_3 leaching process. In Fig. 7, the effects of HNO_3 concentration, solid-to-liquid ratio, and reaction time on the extraction of Fe, Mg, Mo and Ni extraction at 90 °C were plotted. It was observed that the extraction of these elements was positively correlated with HNO_3 concentration and reaction time, while it had a negative relationship with solid-to-liquid ratio. Fe, Mg, Mo, and Ni extraction reached maximum, which were 91.7%, 100%, 89.3%, and 99.7% respectively, under the conditions of using 3 mol L^{-1} HNO_3 as leaching agent, a solid-to-liquid ratio of 1 : 10 g mL^{-1} and a reaction time of 1 hour at 90 °C. The XRF analysis of the residue showed that 99.36% SiO_2, 0.24% MoO_3, and 0.01% Fe_2O_3 were not leached by HNO_3. XRD spectra (Fig. 5) also confirmed that most metal elements were extracted by HNO_3 with only amorphous form left.

$$MoO_3 + 2H^+ \rightarrow MoO_2^{2+} + H_2O \quad (4)$$

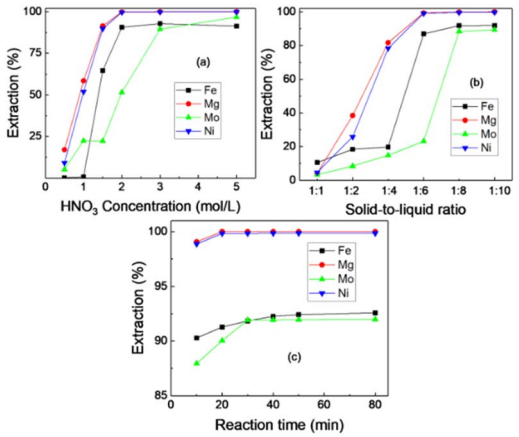

Fig. 7 Effect of HNO_3 concentration (a), solid-to-liquid ratio (b) and reaction time (c).

$$MgO + 2H^+ \rightarrow Mg^{2+} + H_2O \quad (5)$$

$$NiO + 2H^+ \rightarrow Ni^{2+} + H_2O \quad (6)$$

$$Fe_2O_3 + 6H^+ \rightarrow 2Fe^{3+} + 3H_2O \quad (7)$$

3.4 Separation of Mo and Fe from HNO_3 filtrate by liquid–liquid extraction

Filtrate of HNO_3 contains 4.91 g L^{-1} Fe, 2.43 g L^{-1} Mg^{-1}, 1.7 g L^{-1} Mo, and 15.15 g L^{-1} Ni. Solvent extraction method is selected because of its low cost, recyclability of components, high separation coefficient, and capability of continuous operation.[11] Three types of commonly-used extractants were adopted and results were presented in Table 2. P507 and P204 showed good extraction abilities for Fe and Mo, while N235 and TBP extracted nothing. In the acidic medium, molybdenum exists primarily as cationic species. Acidic extractants function by a cation exchange mechanism, where the H^+ from the extractant exchanges with the molybdenum cation in the aqueous phase, forming a neutral, oil–soluble complex that is extracted into the organic phase. This fundamental mechanism explains why acidic extractants are effective here, whereas other types (*e.g.*, basic or solvating extractants) are not suited for these specific cationic Mo species under the given conditions. We chose P507

Table 2 Metal extraction using different extractants[a]

Extractant (volume fraction)		Fe	Mg	Mo	Ni
Alkaline extractant	20% N235	—	—	—	—
Acid extractant	20% P204	62	—	94	—
	20% P507	89	—	98	—
Neutral extractant	20% TBP	—	—	—	—

[a] Extractant. N235: tertiary amine. P204: di-(2-ethylhexyl) phosphoric acid. P507: 2-ethylhexyl phosphoric acid mono-2-ethylhexyl ester. TBP: tri-*n*-butyl phosphate. Diluent: sulfonated kerosene.

to optimize Fe and Mo extraction. The following equations[20] describe the extraction process.

$$2H_3MoO_4^+ + \overline{H_2A_2} \rightarrow 2\overline{H_3MoO_4A} + 2H^+ \quad (8)$$

$$H_6Mo_2O_8^{2+} + \overline{H_2A_2} \rightarrow \overline{H_6Mo_2O_8A_2} + 2H^+ \quad (9)$$

The effect of P507 concentration on Mo and Fe extraction was studied in the range of 6–33 vol% (Fig. 8(a)). It was found that Mo extraction increased from 90.2% to 98.5% and that Fe extraction improved from 45.3% to 96% with increase in P507 concentration. However, the concentration of P507 should not exceed 40% because of its high viscosity.[11] Fig. 8(b) illustrates the extraction of Mo and Fe against extraction time in the system consisting of 20 vol% P507 in SK and the starting solution containing 4.91 g L^{-1} Fe, 2.43 g L^{-1} Mg^{-1}, 1.7 g L^{-1} Mo, and 15.15 g L^{-1} Ni at an O/A ratio of 1 : 1. Mo extraction reached above 97% in less than 5 min, while Fe extraction increased gradually and reached a plateau at 40 min.

Solvent experiment was conducted under optimized conditions of 30 vol% P507 and 40 min extraction time, which achieved 96% Fe extraction and 98.4% Mo extraction. Hydrochloric acid acid (HCl) with concentrations ranging from 2 to 10 mol L^{-1} was used as the stripping agent and results were presented in Fig. 9(a). The iron stripping peaked at 5.5 mol L^{-1} HCl with 87.1% Fe stripping. Mo stripping was less than 0.3% with HCl concentration from 2 to 4 mol L^{-1}. A further increase of HCl concentration to 10 mol L^{-1} resulted in a large increase in Mo extraction. The separation factor ($\beta_{Fe,\ Mo}$) peaked at 4 mol L^{-1} HCl, meaning that Fe and Mo could be perfectly separated under this condition. Therefore, 4 mol L^{-1} HCl was used as the stripping agent, and Fe stripping exceeded 99% after 3 times of the stripping process. $NH_3 \cdot H_2O$ was used as stripping agent for Mo recover from the remaining organic phase (Fig. 9(b)). Mo stripping reached 99.3% with $NH_3 \cdot H_2O$ concentration of 2 mol L^{-1}. The selective stripping of Fe and Mo from the loaded P507 organic phase using HCl and $NH_3 \cdot H_2O$, respectively, can be explained by the distinct aqueous speciation of these metals and the corresponding shift in extraction equilibrium. The high-efficiency stripping of Fe^{3+} with 4 M HCl is achieved by the reversal of the cation-exchange equilibrium driven by high H^+ concentration, coupled with a chloride-induced shift in Fe^{3+} speciation from the extractable $FeCl_4^-$ complex to hydrophilic aqueous species (*e.g.*, $FeCl^{2+}$, $[Fe(H_2O)_6]^{3+}$).[24] In contrast, Mo(VI) forms stable oxychloro

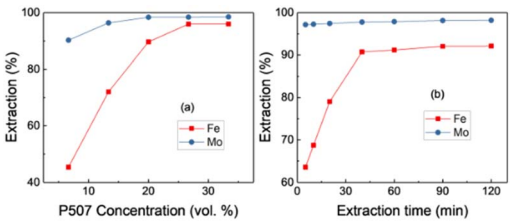

Fig. 8 Effect of P507 concentration (a) and extraction time (b) on Fe and Mo extraction.

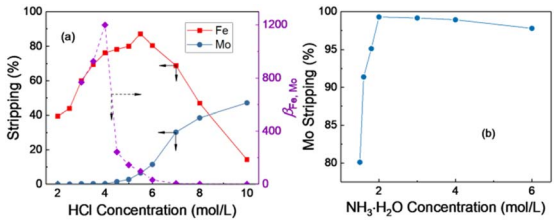

Fig. 9 Fe and Mo stripping by HCl (a) and $NH_3 \cdot H_2O$ (b) solution.

complexes (*e.g.*, MoO_2Cl_2) in HCl media,[25] which remain coordinated to the extractant in 4 M HCl, thus retaining Mo in the organic phase during iron stripping. Subsequently, 2 M $NH_3 \cdot H_2O$ efficiently strips Mo by converting these complexes into the hydrophilic molybdate anion (MoO_4^{2-}),[20] which readily partitions into the aqueous phase.

3.5 Resource utilization

A flow sheet for the resource utilization of spent catalyst was proposed based on the experimental results and demonstrated in Fig. 10. Spent catalyst would go through a two-stage leaching process after pre-processing. 95.8% Mo and 58.1% Si were extracted by NaOH leaching and the filtrate could be used to produce silicomolybdic acid. The second acidic leaching was conducted to extract 91.7% Fe, 100% Mg, 89.3% Mo, and 99.7% Ni from the residue, and then solvent extraction was adopted to separate Mo and Fe from the filtrate. Though a two-stage leaching may complicate hydrometallurgical metal extraction process, the subsequent purification unit is simplified. The proposed process was demonstrated to be a good choice as it enables the attainment of high purity and recovery of products.

A preliminary techno-economic analysis, based on laboratory-scale data, was conducted to assess the potential viability of the process. The estimated consumption of major reagents and utilities per tonne of spent catalyst, alongside the potential revenue from recovered metal products, is summarized in Table 3.

Potential waste streams arising from this process have been preliminarily considered. For instance, the spent eluent from the cation exchange step for sodium removal could be treated to recover sodium salts. The silica-rich residue from the acid precipitation may be explored for valorization in construction materials. The acidic raffinate after solvent extraction, containing Mg and Ni, is intended for the recovery of hydroxide precipitates. Furthermore, process wastewaters from various

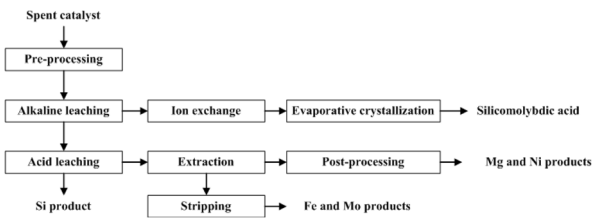

Fig. 10 Flow sheet of resource utilization of spent catalyst.

Table 3 Preliminary economic assessment for processing one tonne of spent catalyst

Category	Item	Estimated quantity	Unit cost (Est.)	Amount (USD)
A. Operating costs	NaOH	1200 kg	0.5 USD kg^{-1}	600
	HNO_3, 65%	2908 kg	0.3 USD kg^{-1}	872
	HCl, 35%	834 kg	0.2 USD kg^{-1}	167
	Ammonia solution, 25%	136 kg	0.4 USD kg^{-1}	54
	Extractant (P507)	40 kg	10.0 USD kg^{-1}	400
	Ion-exchange resin	—	—	200
	Utilities (heating, stirring)	500 kWh	0.1 USD kWh^{-1}	50
	Other consumables	—	—	100
	Operating costs			~2443
B. Potential revenue	Molybdenum	337 kg	30.0 USD kg^{-1}	10 110
	Nickel	275 kg	4.0 USD kg^{-1}	1100
	Iron	17.8 kg	0.5 USD kg^{-1}	9
	Magnesium	10.0 kg	1.0 USD kg^{-1}	10
	Gross revenue			~11 229
C. Key indicator	Estimated gross margin			~8786

stages are planned to be neutralized and recirculated to minimize discharge. These envisaged management strategies aim to address secondary outputs and improve the overall environmental footprint of the recovery process.

4 Conclusions

Extraction of Mo and Si by NaOH leaching was studied, and the optimum parameters were determined to be a reaction time of 2 hours, NaOH concentration of 3 mol L^{-1}, and solid-to-liquid ratio of 1 : 10 g mL^{-1} at 90 °C. In the scale-up experiment, 95.8% Mo and 58.1% Si were extracted, and silicomolybdic acid with only 0.055% Na_2O was produced from NaOH leaching filtrate *via* cation exchange using the resin 732.

NaOH leaching residue was then treated with 3 mol L^{-1} HNO_3 at a solid-to-liquid ratio of 1 : 10 g mL^{-1} and a reaction time of 1 hour at 90 °C. Fe, Mg, Mo and Ni extraction reached maximum, with extraction percentages of 91.7%, 100%, 89.3% and 99.7% respectively. 96% Fe and 98.4% Mo were extracted from the filtrate using 30 vol% P507 and 40 min extraction time. Fe stripping was more than 99% after 3 times of the stripping process adopting 4 mol L^{-1} HCl as stripping agent, while Mo stripping reached 99.3% with 2 mol L^{-1} $NH_3 \cdot H_2O$.

A new hydrometallurgical process for resource utilization of spent catalyst was developed. The process demonstrated high purity and recovery of products, providing potential for industrialization and commercialization. To further advance this technology towards commercialization, the key challenges and corresponding future research directions are outlined as follows:

(1) *Process economics and reagent consumption*: investigate reagent recycling and regeneration (*e.g.*, NaOH, HNO_3, stripping agents); explore cheaper alternative alkali sources or leaching aids; optimize reagent cycles to minimize operational costs.

(2) *Product value and purity of silicon stream*: develop advanced purification techniques (*e.g.*, membrane filtration, recrystallization) for silicon-based products like silicomolybdic acid; explore conversion into higher-value silicon materials or new market applications.

(3) *Waste management and environmental impact*: develop a minimal-waste flow-sheet by valorizing secondary residues (*e.g.*, into construction materials); integrate wastewater treatment and closed-loop water recycling systems; conduct a comprehensive Life Cycle Assessment to benchmark environmental performance.

(4) *Scale-up and continuous operation*: perform continuous pilot-scale trials to address engineering challenges (mixing, heat transfer, solid–liquid separation); design and test corrosion-resistant equipment for harsh process conditions.

Author contributions

Xiaoxue Sun: investigation, conceptualization, methodology, data curation, writing – review & editing; Deju Wang and Junlin Zheng: methodology, review & editing; Renjie Li and Fenglei Xi: data curation, review & editing.

Conflicts of interest

There are no conflicts to declare.

Data availability

Data will be made available on request.

Acknowledgements

This work was financially supported by the National Key R&D Plan (2022YFA1503504) and Shanghai Municipal Commission of Science and Technology Key Technology R&D Program (25ZD3000800).

References

1 C. Yu, S. Yu, L. Li and S. Li, *Fuel*, 2022, **323**, 124334.
2 J. Ji, Y. Bao, X. Liu, J. Zhang and M. Xing, *EcoMat*, 2021, **3**, e12155.

3 Y. Shen, P. Jiang, P. T. Wai, Q. Gu and W. Zhang, *Catalysts*, 2019, **9**, 31.
4 V. Mirjana, B. Francois, G. Gilles, N. L. L. Piet and D. H. Eric, *Leaching and Recovery of Molybdenum from Spent Catalysts, Sustainable Heavy Metal Remediation*, Berlin, Springer International Publishing, 2017.
5 T. A. Fassbach, J. Ji, A. J. Vorholt and W. Leitner, *ACS Catal.*, 2024, **14**, 7289.
6 T. Xie, X. Li, H. Sun and Z. Dan, *Environ. Sci. Pollut. Res.*, 2022, **29**, 63393.
7 V. Gunarathne, A. J. Phillips, A. Zanoletti, A. U. Pajapaksha, M. Vithanage, F. D. Maria, A. Pivato, E. Korzeniewska and E. Bomtempi, *Sci. Total Environ.*, 2024, **912**, 169026.
8 S. A. Saslow, J. R. Hager, C. I. Pearce, T. G. Levitskaia, R. M. Anguish, E. A. Cordova, K. L. Rue, N. M. Escobedo, M. E. Bowden, D. Boglaienko, N. Lahiri, M. H. Engelhard, E. T. Nienhuis, J. Marcial, M. S. Doughman, A. J. Kugler, S. V. Pochampally, L. Gottlieb, M. Carlson and R. D. Mackley, *J. Environ. Chem. Eng.*, 2025, **13**, 116721.
9 C. Soto, N. Toro, S. Gallegos, E. Gálvez, A. Robledo-Cabrera, R. I. Jeldres, M. Jeldres, P. Robles and A. López-Valdivieso, *Materials*, 2022, **15**, 1136.
10 X. Li, T. Wu, Q. Zhou, T. Qi, Z. Peng and G. Liu, *Trans. Nonferrous Met. Soc. China*, 2021, **31**, 842.
11 X. Sun, Z. Liu and W. Yang, *Chem. Ind. Eng. Prog.*, 2016, **35**, 1894.
12 M. Marafi and A. Stanislaus, *Resour., Conserv. Recycl.*, 2008, **52**, 859.
13 M. Marafi and A. Stanislaus, *Resour., Conserv. Recycl.*, 2008, **53**, 1.
14 M. Marafi and A. Stanislaus, *Ind. Eng. Chem. Res.*, 2011, **50**, 9495.
15 R. E. Russo, M. Ventura, M. Fattobene, S. Zamponi, P. Conti, M. Berrettoni and G. Giuli, *ACS Sustainable Chem. Eng.*, 2023, **11**, 15644.
16 K. Chatisa, C. Thanapon, M. Natthicha, Y. Tanongsak, P. Tapany and K. Sakhob, *Mater. Sci. Forum*, 2020, **1009**, 143.
17 Y. Chen, Q. Feng, Y. Shao, G. Zhang, L. Ou and Y. Lu, *Miner. Eng.*, 2006, **19**, 94.
18 K. H. Park, D. Mohapatra and B. R. Reddy, *J. Hazard. Mater.*, 2006, **B138**, 311.
19 R. G. Busnardo, N. G. Busnardo, G. N. Salvato and J. C. Afonso, *J. Hazard. Mater.*, 2007, **B139**, 391.
20 X. Sun, Z. Liu, W. Yang, S. Gu and J. Yu, *Environ. Prog. Sustainable Energy*, 2019, **38**(5), 1.
21 H. Wu, S. Duan, D. Liu, X. Guo, A. Yi and H. Li, *Sep. Purif. Technol.*, 2021, **269**, 118750.
22 W. Mu, S. Shi and Y. Zhai, *Adv. Mater. Res.*, 2013, **813**, 255.
23 D. V. Maiorov, *Theor. Found. Chem. Eng.*, 2025, **59**, 156.
24 S. K. Sharma, *J. Chem. Phys.*, 1974, **60**, 1368.
25 R. Ma, *Extractive Metallurgy*, Beijing, Metallurgical Industry Press, 2009.